Intervertebral Disc Restoration Following Reduced Nucleus Pulposus Glycosaminoglycan in an Animal Model of Early Degeneration

John I. Boxberger, PhD[1,2]
George R. Dodge, PhD[1]
Sounok Sen[1]
Joshua D. Auerbach, MD[1,3]
Nader M. Hebela, MD[1]
Dawn M. Elliott, PhD[1]

[1] Department of Orthopaedic Surgery,
University of Pennsylvania,
Philadelphia PA

[2] Doctors Research Group, Inc.,
Southbury, CT

[3] Department of Orthopaedics,
Bronx-Lebanon Hospital Center,
Albert Einstein College of Medicine,
Bronx, NY

A lack of understanding of the degeneration process has limited treatments aimed at halting or reversing intervertebral disc degeneration. An animal model that replicates key features of human disc degeneration is needed for both elucidating the mechanisms as well as for preclinical testing of therapeutic strategies. The objective of the current work was to investigate the chronic outcomes in an in vivo model in the rat lumbar disc that simulates the diminished glycosaminoglycan and altered mechanics observed in early human disc degeneration. The model had previously been shown to closely resemble early stages of degeneration, yet whether or not the progression to a more severe state occurred was unknown. Rat lumbar intervertebral discs received an injection of a small dose of chondroitinase ABC and evaluated after 24 weeks using microCT to examine disc geometry and abnormal calcifications, disc mechanics, and nucleus glycosaminoglycan content. Additionally, the contribution of aggrecan catabolism was investigated at 4, 12, and 24 weeks through western blots for aggrecan neo-epitope species. Disc height, neutral zone modulus, and range of motion changes that were present at earlier time points were no longer present at 24 weeks. Nucleus glycososaminoglycan remained significantly decreased by 20% relative to controls; however, the magnitude of the decrease was reduced compared to earlier timepoints. The diminished detection of MMP cleaved aggrecan FFGVG fragments after ChABC injection indicates decreased catabolic activity may play a role in the observed restoration of disc properties and function. In summary, an in vivo animal model of early degeneration-like changes was shown to recover towards control levels by 24 weeks. Further work with this model may prove fruitful in defining potential targets for halting or reversing early human degeneration.

Intervertebral disc degeneration is a complex progression of structural, biochemical, and biologic alterations which contribute to compromised mechanical function and in some instances discogenic low back pain. While this highly prevalent disorder is coupled with billions of dollars in health care costs paid annually in United States[1], treatments for disc degeneration and the associated pain are limited largely due to the lack of a thorough understanding of the mechanisms at play during progression. Among the known early degenerative changes is a breakdown of large aggregating proteoglycans, reducing the sulfated glycosaminoglycan content in the nucleus pulposus[2-4]. This in turn impacts the mechanical function of the disc: decreasing the ability of the nucleus pulposus to pressurize which ultimately leads to altered mechanics of the entire motion segment[5-9].

It is likely that progressive degeneration follows reduced glycosaminoglycan content and altered mechanics, yet this ultimately remains a hypothesis, as knowledge of specific mechanisms and interactions at play is limited. To this end, an in vivo animal model simulating the progression of degeneration following decreased nucleus pulposus glycosaminoglycan content would be of great utility. Such a progressive disease model would allow the study of the links between a relevant altered biochemistry, altered mechanical function, and altered cellular function. This might facilitate the development of specific therapies targeted at bolstering anabolic and inhibiting catabolic cellular function, ultimately restoring disc structure and mechanical function.

The experimental reduction of the glycosaminoglycan content in the nucleus is not a new concept as injection of chondroitinase ABC (ChABC) and or other degradative agents into the disc date back over 40 years[10]. We have recently demonstrated that a physiologically relevant reduction of glycosaminoglycans in the nucleus pulposus in the rat lumbar disc over 12 weeks induces changes consistent with human degeneration[11], including loss of pressure and disc height after ChABC injection[12, 13]. This rat model achieves these changes without the necessity for excessive quantities of enzyme sufficient to render discs devoid of glycosaminoglycan chains and without the use of large needle diameters relative to overall disc heights which may act as confounding factors and induce degenerative changes on their own[14-17]. While the rat lumbar spine model has demonstrated utility for understanding the cellular, mechanical, and biochemical alterations following glycosaminoglycan reduction, it ultimately remains unknown whether a chronic degeneration process mimicking human degeneration ensues. The elucidation of such a process would provide a platform for understanding disc degeneration as well as for

Corresponding Author:
Dawn M. Elliott, PhD
Department of Orthopaedic Surgery,
University of Pennsylvania
424 Stemmler Hall,
36th and Hamilton Walk
Philadelphia, PA 19104
delliott@mail.med.upenn.edu

testing novel therapeutics targeted at halting or reversing the progressive disease.

The objective of the current study was to determine the chronic outcomes in an in vivo model in the rat lumbar spine which simulates the diminished glycosaminoglycan and altered mechanics observed in early disc degeneration by using a controlled injection of ChABC via a small diameter needle. We hypothesized that changes in disc height, mechanics, and biochemistry consistent with human degeneration would be observed at 24 weeks after the initial glycosaminoglycan degradation. Specifically, we hypothesized that glycosaminoglycan reduction and the altered biochemical profile would result in progressively decreased disc height (and associated radiographic abnormalities)[18-20], hypermobility (increased axial range of motion and decreased neutral zone modulus), and increased viscoelastic creep strain[21]. Further, it was hypothesized that nucleus and inner annulus glycosaminoglycan contents would progressively decline[2, 22]. Finally, we hypothesized that while the degeneration-like changes in this experimental model initiate from glycanase activity, the chronic cascade may be attributed to elevated aggrecan catabolism relative to anabolism over the 24 week period, evidenced by an increasing presence of degraded aggrecan core protein.

Methods

Study Design

Nineteen male retired breeder Sprague Dawley rats (initial age 7-9 months, weight 483 ± 16g) were included in this IACUC approved study. Animals were assigned to one of two study objectives, the first which investigated the 24 week time point to ascertain whether or not the model resembled chronic disc degeneration via geometrical, mechanical, and biochemical analyses (n = 10). The second objective examined aggrecan structure within the disc over time to identify whether aggrecan breakdown may be playing a role in the observed response (n = 9).

After approximately one week of facility acclimation, rats were operated on using aseptic technique. Rats were anesthetized via inhalation of 1.5-3% isoflurane in an oxygen carrier. Upon reaching appropriate depth of anesthesia, animals were placed in a supine position on a heated pad, and an anterior approach to the lumbar spine was performed, similar to that described previously[11, 23, 24]. The lumbar spine from L3 to S1 was exposed, and a custom 33 gauge needle attached to a gas tight microsyringe (Hamilton Comp, Reno, NV) was inserted through the anterior of the appropriate discs to a controlled depth of 2.5 mm, placing the needle tip in the center of the nucleus pulposus. Within each animal, levels L3/L4, L4/L5, and L5/L6 were randomly assigned to either receive a 1 μL injection of ChABC (Seikagaku, Tokyo, Japan), a 1 μL sham injection of phosphate buffered saline (PBS) with 0.1% bovine serum albumin, or to serve as an intact control. Each ChABC injection contained 0.00025 units of enzyme, prepared to 0.25 U/mL in PBS with 0.1% bovine serum albumin. Musculature adjacent to the ChABC and

sham PBS injection sites was labeled with a metallic marker for post-operative level identification. The abdominal wall was closed, and animal recovery was monitored for adverse symptoms under heated lamp for 45 minutes. Animals were returned to normal housing and received food and water ad libitum. Animals were euthanized via CO_2 inhalation at the appropriate time points, either 4, 12, or 24 weeks post surgery.

Sample Preparation

Immediately after sacrifice, animals were imaged using a fluoroscope (FlouroScan 50700, FluoroScan Imaging Systems, Northbrook, IL) for visualization of the metallic site markers and identification of the ChABC and sham PBS levels. Next, lumbar spines were removed *en bloc* with the ligamentous structures and posterior bony anatomy remaining intact. Spines were wrapped in PBS soaked gauze and frozen at −20°C until samples could be imaged using micro CT.

Micro CT Imaging

Spines for the mechanics/biochemistry assays were removed from −20°C and allowed a 1 hour thaw period followed by 1 hour submersed in a room temperature PBS. Spines then underwent μCT scanning in room temperature PBS at a 42μm isotropic resolution (GE, London, Ontario, Canada). Following scanning all posterior elements were removed and spines were cut into individual bone-disc-bone motion segments. Each motion segment was refrozen at −20°C until mechanical testing. Average disc height, disc area, and total disc volume were calculated from the μCT volumetric data using a custom algorithm (MATLAB, MathWorks, Inc., Natick, MA). In addition to the quantitative geometric measures, qualitative examination for bony abnormalities was performed using Microview software for visualization. Grading was performed by two independent investigators blinded to both time and treatment assignments for each spine. The presence of endplate defects (both voids and bony protrusions), osteophytes on the inferior and superior vertebral bodies, anterior longitudinal ligament calcification, and posterior longitudinal ligament calcification were documented.

Mechanical Testing

Each motion segment was thawed in room temperature PBS for 1 hour. Compression-tension testing was performed at a frequency of 0.1 Hz and ranged from 4.5 N (~0.9x body weight) compression to 3 N tension[5, 25, 26]. This was followed by compressive creep testing which was performed with an applied load of 4.5 N for 45 minutes. Following mechanical testing each motion segment was rehydrated for 1 hour in room temperature PBS and then returned to storage at -20°C until sulfated glycosaminoglycan quantification. Data from the 19th cycle of compression-tension was analyzed using a trilinear fit as described previously[5, 27, 28], where the loading curve was divided into compressive, neutral zone, and tensile regions. Stiffness from each region and total range of motion were obtained and normalized by area and average disc height to obtain apparent modulus and strain values[29, 30].

Glycosaminoglycan Quantification

Discs were isolated from the vertebral bodies via sharp scalpel dissection while frozen. The entire nucleus pulposus was removed from the isolated disc using a hollow 1.5 mm diameter biopsy punch. The entire inner annulus fibrosus was then isolated using a hollow 3.6×2.5 mm elliptical biopsy punch. The remaining peripheral disc tissue was the outer annulus. Tissue wet weight for each region was obtained. Each specimen was dried at 65°C for 24 hours and dry weight obtained. Tissue was digested in 5 mg/mL proteinase K solution at 65°C for 18 hours and analyzed for glycosaminoglycan content using the 1-9 dimethylmethylene blue binding assay.

Western Blotting

Discs undergoing Western blot analysis of aggrecan were removed from the spines while frozen via sharp scalpel dissection. Nucleus and inner annulus samples were isolated as described for the biochemistry analysis above. Tissue was then chopped finely and proteins extracted for a period of 48 hours under constant agitation at 4°C in 4M guanidine HCl containing protease inhibitors (PI) (Complete®, Roche Applied Science, Indianapolis, IN). Samples were placed in dialyzer cassettes with a 10,000 molecular weight cutoff (Pierce Slide-A-Lyzer Mini Dialysis Units, Thermo Scientific, Rockford, IL) and exhaustively dialyzed against distilled H_2O containing 0.1X PI to remove guanidine. Samples were then dried under centrifugation and resuspended in distilled H_2O containing 1X PI. Samples were then digested with 0.01U ChABC at 37°C for 2 hours. After digestion, samples were combined with a concentrated Laemmli sample buffer containing β-mercaptoethanol, run on 4-15% Tris-HCl polyacrylamide gels (Bio-Rad, Hercules, CA), and transferred to supported 0.45 µm nitrocellulose membranes. Membranes were then blocked in 10% non-fat milk in a 1X PBS solution with 0.2% Tween-20. After blocking, membranes were incubated in various primary antibody solutions. A polyclonal aggrecan antibody (AB16320, Abcam, Cambridge, MA) which reacts with the interglobular domain (IGD) of the aggrecan molecule was used at a dilution of 1:2000. Monoclonal antibody specific for unbound FFGVG MMP cleaved fragments (MAB19310, BC-14, Millipore, Billerica, MA) was also utilized on a second set of membranes at a dilution of 1:2000. After primary antibody incubation (2 hours at room temperature), blots were washed and secondary antibodies applied. Appropriate horseradish peroxidase labeled secondary antibodies (Bio-Rad, Hercules, CA) were applied at 1:2000 dilutions in 10% nonfat milk in 1X PBS + 0.2% Tween with a 1 hour room temperature incubation. This was followed by extensive washing with PBS + 0.2% Tween and chemiluminescent detection using SuperSignal West (Thermo Scientific, Indianapolis, IN).

Statistics

A single factor ANOVA (*factor:* treatment, *levels:* intact control, PBS, ChABC) was performed to examine the geometric, mechanical, and biochemical data. Tukey's post hoc tests were utilized to investigate differences between factors. Statistical analyses were performed using SYSTAT 10.2 (SYSTAT Software Inc., San Jose, CA), and significance was set at $p < 0.05$.

Results

Animals tolerated the procedures well, although one animal from the 24 week group died from unknown causes in the 19th week and was excluded from analysis (no adverse symptoms were documented for this animal). All animals maintained or increased body weight throughout the study. Mean body weight after 24 weeks rose to 569 ± 23 g.

Disc Geometry

No significant effects due to treatment were detected for the disc area or volume parameters ($p > 0.05$) after 24 weeks. Disc area remained approximately equivalent to the intact control value of 9.12 ± 1.29 mm^2 in both the sham PBS (9.17 ± 1.13 mm^2) and the ChABC treated discs (9.52 ± 0.69 mm^2). Disc volume, similarly, remained similar to the control value of 8.98 ± 2.17 mm^3 in both the sham PBS (9.17 ± 1.84 mm^3) and ChABC discs (9.37 ± 1.20 mm^3). Average height was likewise not found to be significantly different between groups after 24 weeks with values remaining similar to the control value of 0.973 ± 0.119 mm in both the PBS (0.994 ± 0.094 mm) and the ChABC groups (0.981 ± 0.066 mm).

In addition to being analyzed for disc geometry, micro CT volumes were also graded for the presence of bony deformities. Endplate defects characterized by a void in the endplate and loss of trabecular bone were most prominent in the superior endplate (Figure 1A). Endplate defects were present in 3 discs within the ChABC treated discs, none of the sham PBS injected discs, and in 2 intact control discs. Bony protrusions into the disc from the endplate into the disc space were rare, occurring in only 1 ChABC treated disc. Osteophytes were most prevelant in the anterior of the disc and seemed to be preferentially detected on the superior vertebral body (Figure 1B). Osteophytes were detected in all groups but were most prevalent in both the sham PBS and ChABC discs (7-8 specimens per group) and were detected in just 4 of the intact control discs. In general, osteophytes tended to be larger in the sham PBS and ChABC discs relative to those found in the intact control discs. Calcification of both the anterior and posterior longitudinal ligaments was detected in all groups and did not appear to be continuous with the vertebral bodies (Figure 1C). Within each treatment group, 2-3 occurrences were noted. Ligament calcification was more frequent in the disc anterior as opposed to the posterior, with an occurrence rate of approximately 2:1.

Disc Mechanics

Overall, none of the mechanical measurements in the sham PBS or ChABC groups were different from intact control. Treatment did not have a significant effect on compressive modulus. Values remained no different from the intact control value of 9.90 ± 1.05 MPa in both the sham PBS (9.06 ± 1.70
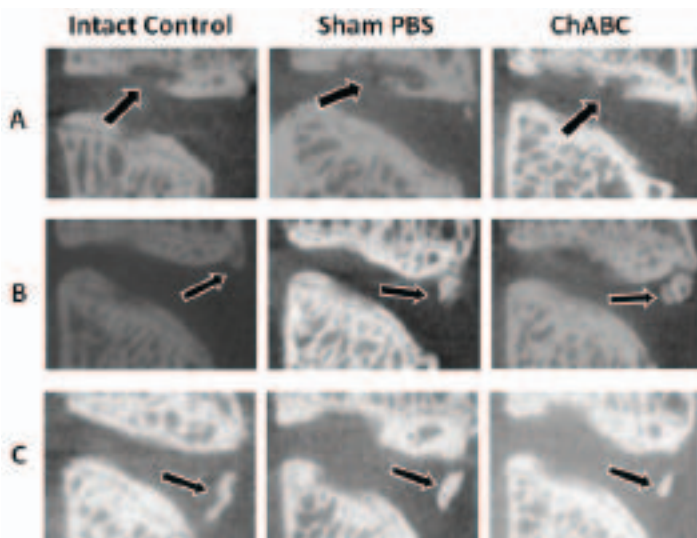
Figure 1. MicroCT analysis revealed endplate defects (A), osteophytes (B), and calcification of the anterior longitudinal ligament (C) in the intact control (left), sham PBS (middle), and ChABC injected discs.

MPa) and the ChABC discs (9.07 ± 1.41 MPa). Similarly, after 24 weeks, no significant differences in tensile or neutral zone modulus values were detected. Values for tensile modulus were 5.74 ± 0.94 MPa in the intact control discs, 4.79 ± 1.44 MPa in the sham PBS discs, and 5.22 ± 0.97 MPa in the ChABC discs. The transitional neutral zone modulus values were 4.43 ± 1.55 MPa in the intact control discs, 3.87 ± 1.58 MPa in the sham PBS discs, and 4.25 ± 0.89 MPa in the ChABC discs. Consistent with modulus values derived from the trilinear analysis, total range of motion strain during loading was unaffected by treatment. Total range of motion strains were 0.16 ± 0.04 mm/mm in the intact control discs, 0.16 ± 0.06 mm/mm in the sham PBS discs, and 0.13 ± 0.03 mm/mm in the ChABC discs. Strain during viscoelastic creep was also not significantly altered by treatment. Values remained similar to the intact control value of 0.18 ± 0.02 mm/mm in both the sham PBS (0.20 ± 0.03 mm/mm) and ChABC groups (0.18 ± 0.03 mm/mm).

Glycosaminoglycan Quantification

Twenty-four weeks after surgery, nucleus pulposus glycosaminoglycan content in the ChABC injected discs remained significantly reduced relative to both intact control and sham PBS by approximately 19% (Table 1). Neither inner annulus glycosaminoglycan content nor outer annulus glycosaminoglycan content were significantly different between treatment groups.

Aggrecan Neo-epitopes

The polyclonal aggrecan antibody positively reacted with a number of aggrecan species, as expected (Figure 2). A high intensity band was detected at approximately 385 kDa (although beyond the standard's precise calibration), likely representing an intact aggrecan molecule. Aggrecan was detected diffusely between approximately 310 kDa and 175 kDa, with a high intensity band at 175 kDa. Another high intensity band was detected at 130 kDa, with two bands of slightly lower intensity at approximately 115 and 105 kDa. Finally, three bands were detected at 65, 60, and 50 kDa. No consistent differences in blot appearance were noted between treatments, or within a treatment across times.

Blots incubated with the FFGVG antibody revealed MMP cleaved aggrecan fragments of heterogeneous molecular weights (Figure 3). The first population of these was between approximately 300 kDa and 190 kDa, with a higher intensity band at 260 kDa. Another grouping was observed between 150 and 110 kDa, with a high intensity band at 130 kDa. At all times, the ChABC injected discs had less MMP cleaved FFGVG aggrecan neo-epitopes, as banding was less intense in both the higher 190-300 kDa range as well as in the lower 110-150 kDa range. The 24 week ChABC discs appeared to have the lowest levels of this fragmented aggrecan, though variability within each time and treatment was high. The PBS sham control samples demonstrated patterns consistent with both ChABC and intact control samples for the polyclonal antibody and with the control samples for the FFGVG antibody (not shown).

Discussion

To date, no animal model has recreated the disc degeneration process as observed in human intervertebral discs. We recently presented an *in vivo* model of early degeneration with reduced nucleus glycosaminoglycan content and altered mechanics, in which degeneration-like changes in disc height, mechanics, and biochemistry are detected at 4 and 12 weeks[11]. It was hypothesized that these effects would be progressive at 24 weeks following surgical intervention. Contrary to what was hypothesized, at 24 weeks, many geometric and mechanical properties which were significantly altered by ChABC induced glycosaminoglycan reduction at 4 and 12

TABLE 1. Glycosaminoglycan content normalized by tissue wet weight and presented as mean (standard deviation) (µg/mg). * Significantly reduced relative to both the intact and sham PBS groups, p < 0.05.

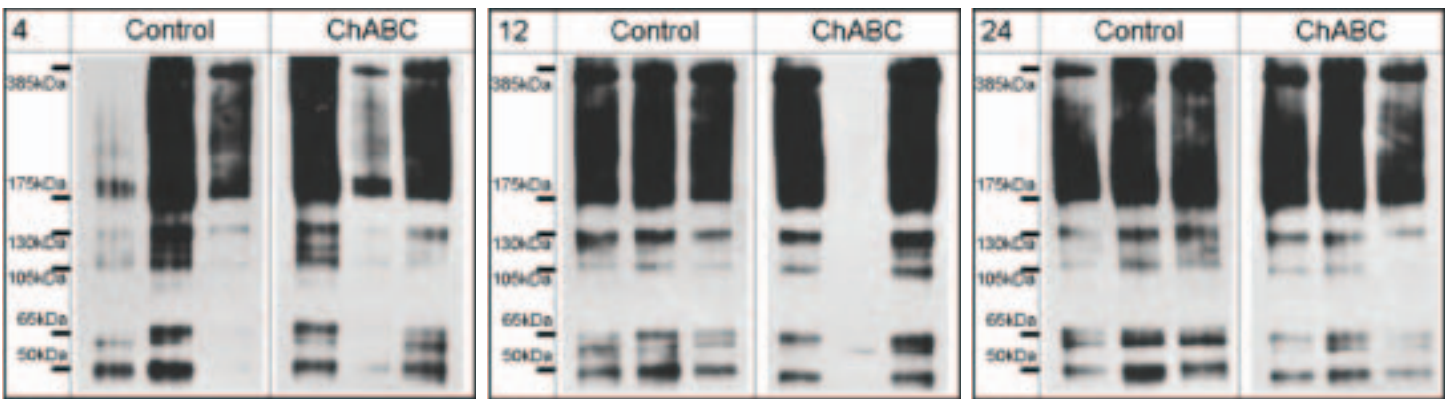|	Intact Control	Sham PBS	ChABC
Nucleus Pulposus	67.3 (8.7)	68.0 (11.6)	54.9 (14.0) *
Inner Annulus	47.7 (7.8)	52.3 (5.0)	44.7 (15.2)
Outer Annulus	15.8 (4.0)	18.3 (4.5)	19.6 (4.9)

Figure 2. Western Blots at 4, 12, and 24 weeks for intact controls (n=3) and ChABC treated (n=3). Figures demonstrate both the banding similarities between treatments as well as the variability between rats within a group.
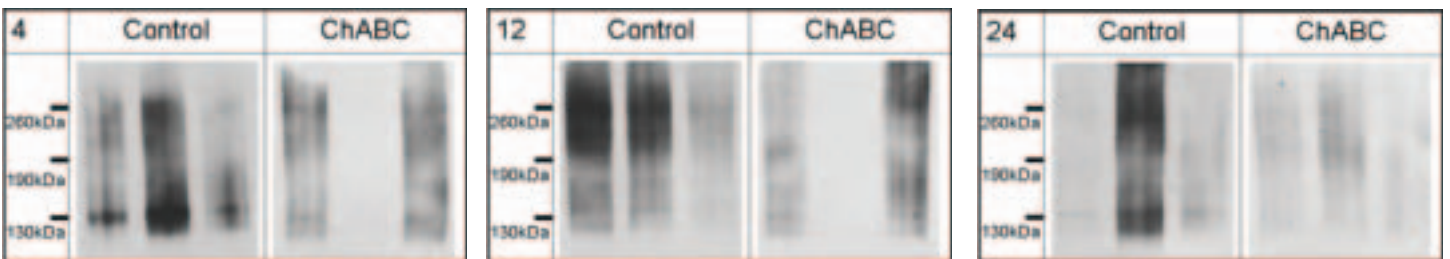

Figure 3. MMP cleaved FFGVG aggrecan fragments at 4, 12, and 24 weeks for intact controls (n=3) and ChABC treated (n=3).

weeks were no longer altered relative to intact control or sham PBS, potentially indicative of disc remodeling. Evidence indicates that the restoration may be attributed partially to a decrease in aggrecan catabolism.

Human disc degeneration is characterized by radiographic observations of reduced disc height[18, 19] and observations of several bony abnormalities. Fracture and defects within the endplates including Schmorl's nodes have been detected in pathologic discs[31]. Further, 73% of patients over 50 years of age had anterior osteophytes while only 37% had disc space narrowing[20]. This is intriguing, as it has long been thought that osteophyte formation occurs in the late stages of disease and as an adaptation to increased shear and compressive deformation and load in attempt to stabilize the joint by better distributing loads[32]. Additionally, ligament calcification has been noted in both the disc anterior and posterior in low incidence rates[33], though it has also been posed that it is ligament calcification that leads to osteophyte formation. In the present work all of these features were identified in the rat discs at 24 weeks (Figure 1). Interestingly, both the endplate defects and ligament calcification appeared equivalently regardless of treatment (intact, PBS, or ChABC). It is likely that the endplate defects are due to natural aging and are likely to occur in a percentage of the rat population by the ages of approximately 8-15 months. The ligament calcification may also be related to natural aging or be a result of the surgical exposure, as even intact controls were exposed anteriorly. Overall, it is likely that the radiographic signs typically associated with a degenerative disc may be due to natural aging or the surgical exposure in this model.

The mechanical function of the disc is altered during the progression of degeneration. In early degeneration the motion segment exhibits a reduced stiffness, though by late degeneration stiffness returns largely due a loss of disc height. Motion segment mechanics are altered by the interaction of alterations in nucleus and annulus biochemistry and mechanics. The decreased nucleus pressure due to glycosaminoglycan loss[34] contributes to an increase in hypermobility of the entire motion segment[27, 35], likely responsible for the early degenerative reduction in stiffness. Alterations in disc viscoelasticity occurring during degeneration, including increased creep and creep rate[36, 37], can also be partly attributed to reduced nucleus glycosaminoglycan[38]. By late degeneration viscoelastic mechanics tend to return towards healthy levels, again likely influenced by the changing morphometry of the disc space. The initially increased hypermobility and creep may contribute to mechanical progression of degeneration as the resulting alterations in local stress and strain lead to damage accumulation. The later recovery of mechanical properties is likely multifactorial, but may be in response to protective disc remodeling in order to reduce the aberrant stresses and strains. In the model presented here, changes in height and mechanical properties consistent with the early stages of degeneration including hypermobility were observed at the 4 and 12 week timepoints (Figure 4 and 5)[11]. Additionally, altered viscoelastic creep behavior was detected early after the intervention. Over time, however, the disc height and mechanical properties returned towards control levels (Figure 4 and 5). The recovery observed in this model is a material change and likely due to disc matrix remodeling and disc recovery as opposed to advanced degeneration process.
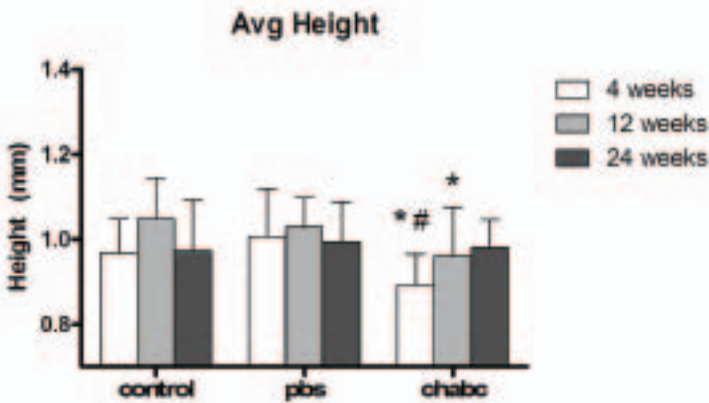
Figure 4. Average (standard deviation) disc height at 4 (white), 12 (light grey), and 24 (dark grey) weeks. The initial height loss at 4 weeks following ChABC treatment returns to control values by 24 weeks. The 4 and 12 week results were previously published[11]. * significant difference compared to intact control; # significant difference compared to PBS.
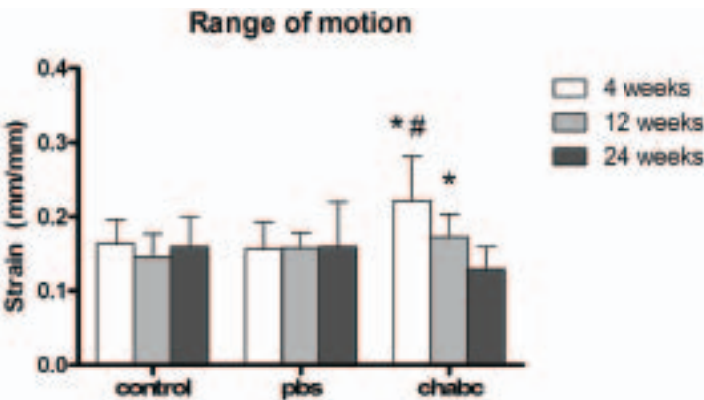

Figure 6. Average nucleus pulposus glycosaminoglycan content at 4 (white), 12 (light grey), and 24 (dark grey) weeks. The initial glycosaminoglycan loss at 4 weeks following ChABC treatment returns toward control values but remains below control values at 24 weeks. The 4 and 12 week results were previously published[11]. * significant difference compared to intact control; # significant difference compared to PBS.

Figure 5. Average range of motion at 4 (white), 12 (light grey), and 24 (dark grey) weeks. The initial hypermobility at 4 weeks following ChABC treatment returns to control values by 24 weeks. The 4 and 12 week results were previously published[11]. * significant difference compared to intact control; # significant difference compared to PBS.

Biochemically, during the process of degeneration, the first detectable changes are a reduction in nucleus pulposus glycosaminoglycan content through the degradation of aggrecan molecules. Nucleus glycosaminoglycan is reduced by upwards of 50% in the early to mid stages of disease and by up to 90% in advanced degeneration[2, 22]. Accompanying this change is a decline in water content and an increase in type I collagen within the nucleus. The annulus also undergoes biochemical changes including reduced glycosaminoglycan in the inner regions. Along with accumulation of denatured collagens, there is an increase in non-enzymatic glycation end products and collagen crosslinking during the degeneration process[39, 40]. Though the model here indicated early degeneration-like changes of reduced nucleus and inner annulus glycosaminoglycan at 4 and 12 weeks, this reduction did not progressively increase in magnitude during the time course, as demonstrated in Figure 6. To the contrary, mean nucleus glycosaminoglycan values tended to increase in the ChABC injected discs over time, though levels still remained significantly reduced relative to controls by the 24 week time point. This difference may be related to a failure in the model to induce the concurrent biochemical changes
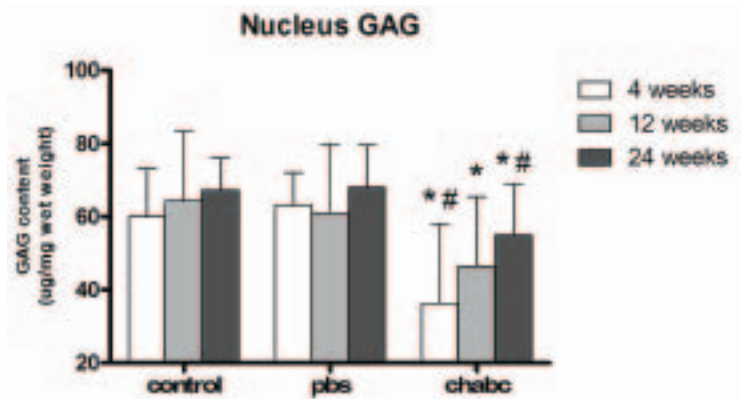
associated with degeneration which may be required for disease progression. The associated changes in disc collagens were not measured here.

Few studies have investigated aggrecan fragmentation in the disc, though it has been commonly put forth that both bound (to hyaluronan) and unbound fragments remain in the tissue due to the poor diffusion characteristics and contained nature of the disc[41]. There is an increased presence of various MMPs in discs with higher degenerative grade[42]. Moreover, active ADAMTS-4 is present in severely degenerate discs at elevated levels versus moderately degenerate discs[43]. It is therefore not surprising that aggrecan fragments resulting from both MMPs and aggrecanases have been detected in the nucleus pulposus late into adulthood[44]. In the present work, varying IGD containing aggrecan species as well as MMP derived FFGVG neo-epitopes were positively detected in the rat intervertebral disc. The molecular weights of these fragments were consistent with published data and expected sizes for aggrecan[45]. A fully intact, bound molecule, has been reported to have a molecular weight of approximately 350 kDa[45], and species resulting from core molecule cleavage would be expected to range in size from that of a nearly intact molecule to the size of an MMP cleaved G1-DIPEN[341] containing fragment, 52 kDa[46]. Indeed, species between 310 and 105 kDa were detected with both the IGD detecting antibody and the MMP cleaved neo-epitope antibody. Additionally, IGD containing fragments were detected between 65 and 50 kDa, which is consistent with both NITEGE and VDIPEN fragments, though neither were positively identified with specific monoclonal antibodies in this study.

No apparent differences in the overall profile of IGD containing aggrecan were identified due to either treatment or time; however, a decrease in the detection of MMP generated FFGVG neo-epitopes was observed in the ChABC injected discs at all time points. This indicates a potential decrease in catabolism within the nucleus pulposus. The decrease may be the result of a decreased presence of MMPs or a potential decrease in MMP activity. Further, the findings may be the result of the increased presence of MMP inhibitors and elevated inhibitor activity. Finally, the decrease may be the

result of further processing of the molecules by aggrecanases, such as at the NITEGE-ARGSV site, which would remove the FFGVG neoepitope from remainder of the fragment. The decrease, however, does not appear to be due to a decreased overall presence of aggrecan, as no noticeable differences were noted between treatments or times. Taken together with the previous findings of increasing nucleus glycosaminoglycan content over time in the ChABC injected nucleus (Figure 6), it can be postulated that decreased catabolism is responsible for the decrease in aggrecan fragments.

As with any *in vivo* model of disc degeneration, this model of glycosaminoglycan reduction followed by mechanical and geometric recovery is not without limitations. The use of multiple treatments in adjacent segments within the same spines may complicate the findings. Further, the biologic response following glycosaminoglycan reduction via ChABC treatment may vary from that seen after MMP- and aggrecanase-mediated aggrecan cleavage and lysosomal glycosaminoglycan degradation, as occurs naturally. Further, it is likely that the degenerative change of glycosaminoglycan reduction occurs in concert with other changes to the disc matrix, which were not incorporated into this model. Nonetheless, this specifically dosed ChABC model provided the unique ability to reduce nucleus glycosaminoglycan content by a controlled amount.

In summary, this and previous work demonstrates an *in vivo* model of nucleus pulposus glycosaminoglycan reduction in the rat lumbar spine, which at 4 weeks after surgery produces discs which morphometrically, mechanically, and biochemically resemble early degenerating human intervertebral discs. However, over a 24 week period following surgery, the biochemically altered discs appear to undergo remodeling and restoration of these same morphometric, mechanical, and biochemical properties. A decrease in aggrecan catabolism may be contributing to this restoration of properties towards control levels. The need still remains for an animal model of intervertebral disc degeneration which mimics the human process. While the model presented here did not progressively degenerate, the observed recovery may be of significant interest in developing future therapies targeted at restoring disc function. Knowledge of the cellular mechanisms at play in this response may yield insight into means for combating the intervertebral disc degeneration process.
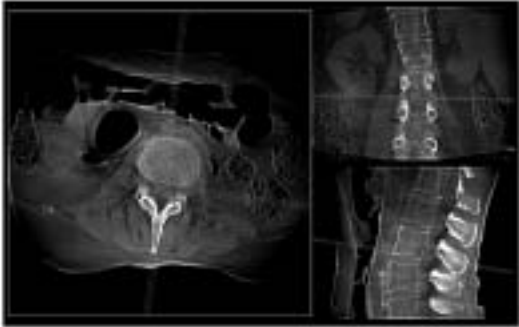
Acknowledgements

References

1. **Luo X, Pietrobon R, Sun SX, Liu GG, Hey L.** Estimates and patterns of direct health care expenditures among individuals with back pain in the United States. *Spine.* 2004;29(1):79-86.

2. **Antoniou J, Steffen T, Nelson F, Winterbottom N, Hollander AP, Poole RA, et al.** The human lumbar intervertebral disc: evidence for changes in the biosynthesis and denaturation of the extracellular matrix with growth, maturation, ageing, and degeneration. *Journal of Clinical Investigation.* 1996;98(4):996-1003.

3. **Pearce RH, Grimmer BJ, Adams ME.** Degeneration and the chemical composition of the human lumbar intervertebral disc. *Journal of Orthopaedic Research.* 1987;5(2):198-205.

4. **Roughley PJ, Alini M, Antoniou J.** The role of proteoglycans in aging, degeneration and repair of the intervertebral disc. *Biochemical Society Transactions.* 2002;30(Pt 6):869-74.

5. **Boxberger JI, Sen S, Yerramalli CS, Elliott DM.** Nucleus pulposus glycosaminoglycan content is correlated with axial mechanics in rat lumbar motion segments. *Journal of Orthopaedic Research.* 2006;24(9):1906-15.

6. **Iatridis JC, Setton LA, Weidenbaum M, Mow VC.** Alterations in the mechanical behavior of the human lumbar nucleus pulposus with degeneration and aging. *Journal of Orthopaedic Research.* 1997;15(2):318-22.

7. **Johannessen W, Vresilovic EJ, Mills JR, Cloyd JM, Guerin HL, Elliott DM.** Effect of nucleotomy on tension-compression behavior of the intervertebral disc. *Transactions of the Orthopaedic Research Society.* 2005;51:1587.

8. **Perie DS, Maclean JJ, Owen JP, Iatridis JC.** Correlating material properties with tissue composition in enzymatically digested bovine annulus fibrosus and nucleus pulposus tissue. *Annals of Biomedical Engineering.* 2006;34(5):769-77.

9. **Boxberger JI, Orlansky AS, Sen S, Elliott DM.** Reduced nucleus pulposus glycosaminoglycan content alters intervertebral disc dynamic viscoelastic mechanics. *J Biomech.* 2009 Jun 17.

10. **Saunders EC.** Treatment of the canine intervertebral disc syndrome with chymopapain. *Journal of the American Veterinary Medical Association.* 1964;145:893-6.

11. **Boxberger JI, Auerbach JD, Sen S, Elliott DM.** An in vivo model of reduced nucleus pulposus glycosaminoglycan content in the rat lumbar intervertebral disc. *Spine.* 2008;33(2):146-54.

12. **Sasaki M, Takahashi T, Miyahara K, Hirose AT.** Effects of chondroitinase ABC on intradiscal pressure in sheep: an in vivo study. *Spine.* 2001;26(5):463-8.

13. **Yamada K, Tanabe S, Ueno H, Oinuma A, Takahashi T, Miyauchi S, et al.** Investigation of the short-term effect of chemonucleolysis with chondroitinase ABC. *Journal of Veterinary Medical Science.* 2001;63(5):521-5.

14. **Kim KS, Yoon ST, Li J, Park JS, Hutton WC.** Disc degeneration in the rabbit: a biochemical and radiological comparison between four disc injury models. *Spine.* 2005;30(1):33-7.

15. **Masuda K, Aota Y, Muehleman C, Imai Y, Okuma M, Thonar E, et al.** A novel rabbit model of mild, reproducible disc degeneration by an anulus needle puncture: correlation between the degree of fisc injury and radiological and histological appearances of disc degeneration. *Spine.* 2005;30(1):5-14.

16. **Sobajima S, Kompel JF, Kim JS, Wallach CJ, Robertson DD, Vogt MT, et al.** A slowly progressive and reproducible animal model of intervertebral disc degeneration characterized by MRI, X-ray, and histology. *Spine.* 2005;30(1):15-24.

17. **Elliott DM, Yerramalli CS, Beckstein JC, Boxberger JI, Johannessen W, Vresilovic EJ.** The effect of relative needle diameter in puncture and sham injection animal models of degeneration. *Spine.* 2008 Mar 15;33(6):588-96.

18. **Pfirrmann CW, Metzdorf A, Elfering A, Hodler J, Boos N.** Effect of aging and degeneration on disc volume and shape: A quantitative study in asymptomatic volunteers. *Journal of Orthopaedic Research.* 2006;24(5):1086-94.

19. **Benneker LM, Heini PF, Anderson SE, Alini M, Ito K.** Correlation of radiographic and MRI parameters to morphological and biochemical assessment of intervertebral disc degeneration. *European Spine Journal.* 2005;14(1):27-35.

20. **Pye SR, Reid DM, Lunt M, Adams JE, Silman AJ, O'Neill TW.** Lumbar disc degeneration: association between osteophytes, end-plate sclerosis and disc space narrowing. *Ann Rheum Dis.* 2007 Mar;66(3):330-3.

21. **Brown MD, Holmes DC, Heiner AD.** Measurement of cadaver lumbar spine motion segment stiffness. *Spine.* 2002;27(9):918-22.

22. **Keshari KR, Lotz JC, Kurhanewicz J, Majumdar S.** Correlation of HR-MAS spectroscopy derived metabolite concentrations with collagen and proteoglycan levels and Thompson grade in the degenerative disc. *Spine.* 2005;30(23):2683-8.

23. **Gruber HE, Johnson TL, Leslie K, Ingram JA, Martin D, Hoelscher G, et al.** Autologous intervertebral disc cell implantation: a model using Psammomys obesus, the sand rat. *Spine.* 2002;27(15):1626-33.

24. **Rousseau MA, Bass EC, Lotz JC.** Ventral approach to the lumbar spine of the Sprague-Dawley rat. *Lab Animal.* 2004;33(6):43-5.

25. **Elliott DM, Sarver JJ.** Young investigator award winner: validation of the mouse and rat disc as mechanical models of the human lumbar disc. *Spine.* 2004;29(7):713-22.

26. **Yerramalli CS, Chou AI, Miller GJ, Nicoll SB, Chin KR, Elliott DM.** The effect of nucleus pulposus crosslinking and glycosaminoglycan degradation on disc mechanical function. *Biomechanics & Modeling in Mechanobiology.* 2007;6(1-2):13-20.

27. **Johannessen W, Cloyd JM, O'Connell GD, Vresilovic EJ, Elliott DM.** Trans-endplate nucleotomy increases deformation and creep response in axial loading. *Annals of Biomedical Engineering.* 2006;34(4):687-96.

28. **Sarver JJ, Elliott DM.** Mechanical differences between lumbar and tail discs in the mouse. *Journal of Orthopaedic Research.* 2005;23(1):150-5.

29. **O'Connell GD, Vresilovic EJ, Elliott DM.** Comparison of animals used in disc research to human lumbar disc geometry. *Spine.* 2007 Feb 1;32(3):328-33.

30. **Beckstein JC, Sen S, Schaer TP, Vresilovic EJ, Elliott DM.** Comparison of animal discs used in disc research to human lumbar disc: axial compression mechanics and glycosaminoglycan content. *Spine.* 2008 Mar 15;33(6):E166-73.

31. **Yasuma T, Saito S, Kihara K.** Schmorl's nodes. Correlation of X-ray and histological findings in postmortem specimens. *Acta Pathol Jpn.* 1988 Jun;38(6):723-33.

32. **Macnab I.** The traction spur. An indicator of segmental instability. *J Bone Joint Surg Am.* 1971 Jun;53(4):663-70.

33. **Firooznia H, Rafii M, Golimbu C, Tyler I, Benjamin VM, Pinto RS.** Computed tomography of calcification and ossification of posterior longitudinal ligament of the spine. *J Comput Tomogr.* 1984 Oct;8(4):317-24.

34. **Johannessen W, Elliott DM.** Effects of degeneration on the biphasic material properties of human nucleus pulposus in confined compression. *Spine.* 2005;30(24):E724-9.

35. **Cannella M, Arthur A, Allen S, Keane M, Joshi A, Vresilovic E, et al.** The role of the nucleus pulposus in neutral zone human lumbar intervertebral disc mechanics. *Journal of Biomechanics.* 2008;41(10):2104-11.

36. **Keller TS, Spengler DM, Hansson TH.** Mechanical behavior of the human lumbar spine. I. Creep analysis during static compressive loading. *Journal of Orthopaedic Research.* 1987;5(4):467-78.

37. **Kazarian LE.** Creep characteristics of the human spinal column. *Orthopedic Clinics of North America.* 1975;6(1):3-18.

38. **Keller TS, Hansson TH, Holm SH, Pope MM, Spengler DM.** In vivo creep behavior of the normal and degenerated porcine intervertebral disk: a preliminary report. *Journal of Spinal Disorders.* 1988;1(4):267-78.

39. **Duance VC, Crean JK, Sims TJ, Avery N, Smith S, Menage J, et al.** Changes in collagen cross-linking in degenerative disc disease and scoliosis. *Spine.* 1998;23(23):2545-51.

40. **Pokharna HK, Phillips FM.** Collagen crosslinks in human lumbar intervertebral disc aging. *Spine.* 1998;23(15):1645-8.

41. **Roughley PJ, Melching LI, Heathfield TF, Pearce RH, Mort JS.** The structure and degradation of aggrecan in human intervertebral disc. *Eur Spine J.* 2006 Aug;15 Suppl 15: 326-32.

42. **Roberts S, Caterson B, Menage J, Evans EH, Jaffray DC, Eisenstein SM.** Matrix metalloproteinases and aggrecanase: their role in disorders of the human intervertebral disc. *Spine.* 2000;25(23):3005-13.

43. **Patel KP, Sandy JD, Akeda K, Miyamoto K, Chujo T, An HS, et al.** Aggrecanases and aggrecanase-generated fragments in the human intervertebral disc at early and advanced stages of disc degeneration. *Spine* 2007 Nov 1;32(23):2596-603.

44. **Sztrolovics R, Alini M, Roughley PJ, Mort JS.** Aggrecan degradation in human intervertebral disc and articular cartilage. *Biochem J.* 1997 Aug 15;326 (Pt 1):235-41.

45. **Lemons ML, Sandy JD, Anderson DK, Howland DR.** Intact aggrecan and fragments generated by both aggrecanse and metalloproteinase-like activities are present in the developing and adult rat spinal cord and their relative abundance is altered by injury. *J Neurosci.* 2001 Jul 1;21(13):4772-81.

46. **Struglics A, Larsson S, Pratta MA, Kumar S, Lark MW, Lohmander LS.** Human osteoarthritis synovial fluid and joint cartilage contain both aggrecanase- and matrix metalloproteinase-generated aggrecan fragments. *Osteoarthritis Cartilage.* 2006 Feb;14(2):101-13.